Interface vibrational modes and interface structure of CdSe/ZnTe superlattices

Y. Jin, G. G. Siu, and M. J. Stokes
Department of Physics and Materials Science, City University of Hong Kong, Tat Chee Avenue, Kowloon, Hong Kong, China

S. L. Zhang
Department of Physics, Peking University, Beijing 100871, People's Republic of China

(Received 3 February 1997)

Interfacial vibrational modes (IFM's) of CdSe/ZnTe superlattice are shown for perfect and atomically rearranged interfaces with four probable exchange configurations. In addition to the IFM at 222 cm^{-1} originating from single interface Zn-Se ''wrong'' bonds (WB's), another IFM at 235 cm^{-1} occurs due to atomic rearrangement at the interfaces, which is attributed to double Zn-Se WB's. Raman scattering on both atomic-layer-epitaxy and molecular-beam-epitaxy grown samples is reported. Using the experimental data for the 218 cm^{-1} line of LIF as a base for improving calculations, the corresponding LIF_2 line is predicted at 228 cm^{-1}. Experiments failed to detect this line owing to insufficient double WB's with long-range order. This characteristic IFM is observed in an annealed sample, with abnormally strong intensity at 227 cm^{-1}. [S0163-1829(98)01903-1]

I. INTRODUCTION

CdSe/ZnTe superlattice (SL) is a lattice-matched heterostructure since the lattice parameters of cubic CdSe and ZnTe are closely matched, 6.099 and 6.077 Å, respectively. It is also the only II-VI system formed between two binary compounds without common anions or cations. Raman scattering studies on CdSe/ZnTe SL (Ref. 1) show an interfacial vibrational mode (IFM) at the interface between the CdSe and ZnTe layers, which is attributed to the stretching of a localized Zn-Se bond whose multiphonons up to fifth order are observed.[2] The order and temperature dependencies of the multiphonon linewidth show that the IFM is defectlike. The Zn-Se IFM is a two-dimensional analogue of the vibrational modes of point defects in bulk three-dimensional (3D) semiconductors.[2] In general, at the interfaces between the AB and CD layers of an AB/CD SL, the cross-interface bonds of A-D and C-B are distinct from the A-B and C-D bonds owing to the lack of common anions or cations. These are referred to as wrong bonds (WB's). Their vibrational modes evanesce exponentially toward both layers and hence localize at the interface. Raman scattering can detect these IFM's (Refs. 1–10) that thus serves as a spectroscopic probe for interface structure in order to understand fundamental growth processes.

Recently, atomic rearrangement during growth at CdSe/ZnTe interfaces, shown by x-ray diffraction (XRD), x-ray-absorption fine-structure spectroscopy (XAFS), and transmission-electron microscopy (TEM) (Ref. 11) on molecular-beam-epitaxy (MBE) grown samples, has aroused concern about the interfacial structure of CdSe/ZnTe SL. This is of prime importance for the vibration properties[3] and electronic band structure[6] of the SL. Four possible reordering configurations across interfaces have been proposed.[11] Could they also be characterized by Raman scattering?

In this work, the dynamic properties of CdSe/ZnTe SL are first theoretically studied for perfect and atomic reordered interfaces and characteristic IFM's including one of atomic rearrangement, are determined. Raman scattering is then applied to both the atomic-layer-epitaxy (ALE)- and MBE-grown CdSe/ZnTe SL's. Besides the IFM that originates from single Zn-Se WB's a second IFM that originates from double Zn-Se WB's is observed and identified.

II. EXPERIMENTATION

SL's $(CdSe)_4/(ZnTe)_8$, $(CdSe)_8/(ZnTe)_{12}$, and $(CdSe)_{10}/(ZnTe)_{10}$, which consist of less than a hundred periods,[1] were grown by ALE at 220 °C on a (001) GaAs substrate with a 2 μm (001) ZnTe buffer layer. This serves to decrease the dislocation density owing to the 7% lattice mismatch between ZnTe and GaAs. The details of the growth conditions are given elsewhere.[12] Another four samples similar to those prepared and investigated in Ref. 11, were grown by MBE at 310 °C, and provided by Furdyna and Yang. The four SL's $(CdSe)_m/(ZnTe)_n$ are labeled as M_i $(i=1-4)$, respectively, for (1) $m=n=6$; (2) $m=n=4$; (3) $m=5$, $n=3$; and (4) $m=n=2$.

Raman spectra were taken at liquid-nitrogen temperature. The backscattering geometry of $z(x',x')z$ configuration from the (001) surface was employed, where x' and z are the [110] and [001] directions of the underlying zinc-blende structure, respectively. Excitation was provided by the Ar^+ laser lines and the RAMALOG 1403 spectrometer system was used with a cooled photomultiplier tube detector, Hamamatsu R928.

III. THE LINEAR-CHAIN MODEL

Figure 1 is a schematic plot of a $(CdSe)_4/(ZnTe)_8$ SL. Each atom row follows the convention of a linear chain, with all possible interface configurations: sharp interface S and four atomic rearrangements R_1, R_2, R_3, and R_4. There are two types of interfaces: (I) the Zn-Se interface and (II) the

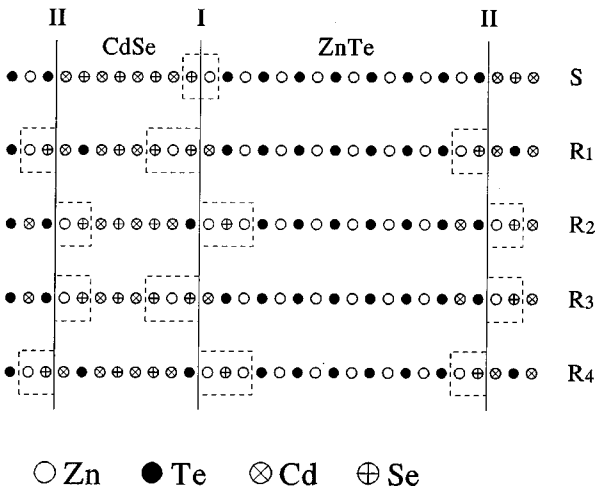

FIG. 1. Schematic plot of $(CdSe)_4/(ZnTe)_8$ SL: S for a sharp interface, R_i $(i=1-4)$ are four configurations of atomic rearrangement. The nominal interfaces are presented by vertical lines: I and II are the light (Zn-Se) and heavy (Cd-Te) interfaces, respectively. Zn-Se WB's are boxed with dashed line. Each row of ions follows the convention of the linear chain model.

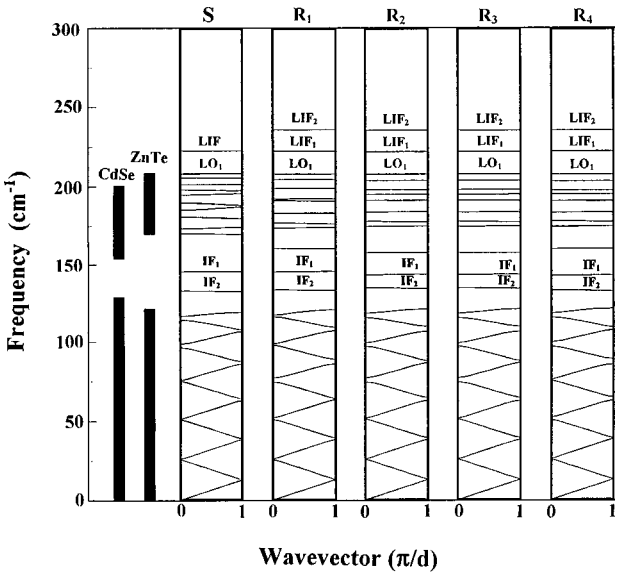

FIG. 2. The dispersion curves of longitudinal phonons along the [001] direction in a $(CdSe)_4/(ZnTe)_8$ SL for S and R_i $(i=1-4)$ configurations. Longitudinal phonon continua of both materials are shown on the left.

Cd-Te interfaces. The four possible rearrangements are R_1, the switch of cations across interface I while anions exchange across interface II; R_2, the switch of anions across I while cations exchange across II; R_3, only the cations switch across both interfaces I and II, R_4, only the anions exchange across both interfaces I and II.

These are limited to the nearest two atomic planes at the interface.[11] The configurations show that atomic reordering is rigorous, implying some correlation between interfaces I and II. It is readily seen that there are two kinds of single WB's, Zn-Se and Cd-Te, alternatively appearing at interfaces I and II in the S configuration. Exchange of interface atomic planes introduces not only single WB's but also double WB's such as Zn-Se-Zn or Se-Zn-Se (Zn-Se double WB), Cd-Te-Cd or Te-Cd-Te (Cd-Te double bond) to SL. All Zn-Se WB's are boxed by the dashed line in Fig. 1. In atomic rearranged interfaces, WB's never cross over the interfaces and do not locate at the nominal interface as in the S configuration.

The linear chain model with the nearest-neighbor approximation[13] is used to calculate the dispersion curve of longitudinal phonons of the $(CdSe)_4/(ZnTe)_8$ SL along the [001] direction. The parameters are the same as in Table I of Ref. 1. All force constants, including those of Zn-Se and Cd-Te, are obtained by fitting to the corresponding bulk values of the longitudinal-optical (LO) phonon frequencies at the Γ point.[14,15] Calculated dispersion curves are shown in Fig. 2 for cases S and R_i $(i=1,2,3,4)$, respectively. The longitudinal phonon continua (bands) of both ZnTe and CdSe compounds are also shown for comparison. The S dispersion curves have been discussed in Ref. 1. Three modes, denoted as interfacial (IF), lie beyond the phonon branches of either ZnTe or CdSe. The topmost one at 222 cm^{-1} (above the optical branches) is a strong Zn-Se IFM strongly localized to the interface,[1] denoted as LIF. Its maximum frequency originates from the larger force constant of the Zn-Se bond and smaller reduced mass compared to other bonds. Two other modes lie in the gap between the optical and acoustic branches of either ZnTe or CdSe, labeled as IF_1 and IF_2.

For the R_i dispersion curves there are still two gap modes IF_1 and IF_2, but on the top of the optical bands two interface modes appear, labeled as LIF_1 and LIF_2. These modes are at nearly the same frequencies. LIF_1 is at 222 cm^{-1}, coincident with that of LIF and LIF_2 at 235 cm^{-1}. For the assignment of LIF_1 and LIF_2, the displacement patterns of R_i are calculated from the linear-chain model. In all four cases, LIF_1 is a localized IFM of Zn-Se single WB and LIF_2 is a localized IFM of Zn-Se double WB, although their locations depend on the specific arrangement. This explains the frequency coincidence of LIF and LIF_1 (henceforth the subscript 1 will be eliminated). The IFM of Zn-Se double WB has an upward frequency shift of 13 cm^{-1} from LIF owing to the more bulklike environment of its innermost ion—Se in configurations R_1 and R_3, Zn in R_2 and R_4 (Fig. 1). Furthermore, IF_1 and IF_2 can be assigned to in-phase motion of Zn-Se and out-of-phase motion of Cd-Te, respectively. In retrospect it is concluded that LIF_2 is the characteristic of interface rearrangement of CdSe/ZnTe SL.

IV. THE BOND POLARIZABILITY MODEL

It is well established that in a semiconductor SL with underlying zinc-blende structure the longitudinal phonons propagating along the [001] direction are all Raman active in backscattering geometry.[16] However, the observability depends on their scattering efficiency. To determine whether LIF_2 can be detected, the Raman scattering intensity of LIF_2 is calculated, together with those of LIF and the ZnTe confined mode LO_1, using the bond polarizability model[16,17] that has already been applied to the II-VI heterostructure (ZnSe/ZnTe SL).[18]

Let x, y denote crystalline axes and A denote a bond. The

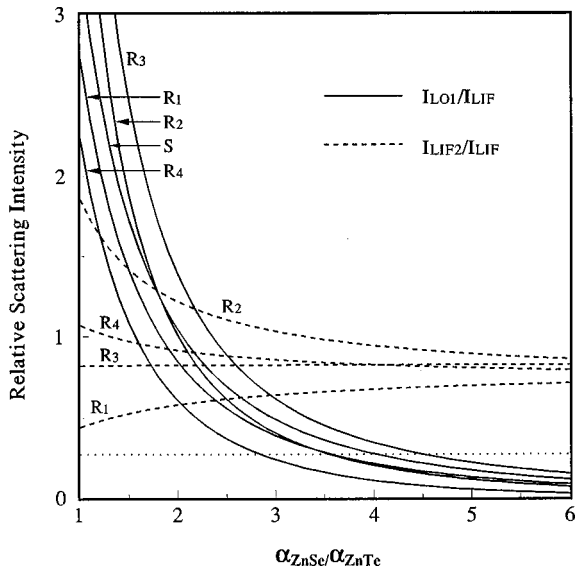

FIG. 3. Curves of relative intensity I_{LO_1}/I_{LIF} (solid) and I_{LIF_2}/I_{LIF} (dashed) vs the ratio $\alpha_{ZnSe}/\alpha_{ZnTe}$ for the configurations S and R_i $(i=1-4)$. The horizontal line (dotted) represents the experimental value of $I_{LO_1}/I_{LIF}=0.27$.

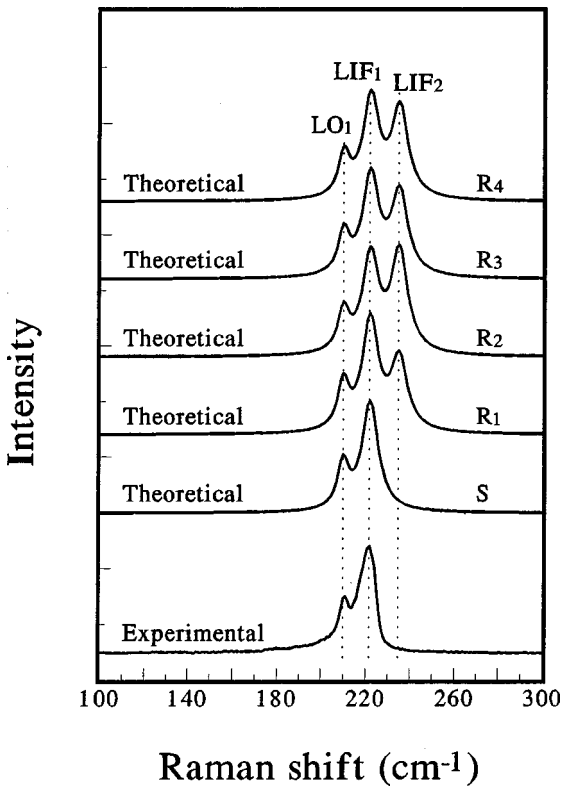

FIG. 4. Raman spectra of $(\underline{Cd}Se)_4/(ZnTe)_8$ SL measured in backscattering geometry of $z(x',x')\bar{z}$ configuration: five spectra from top downward are simulated ones for S and R_i $(i=1-4)$ configurations: the bottom spectrum is the experimental one of the ALE grown SL excited by 501.7-nm line.

polarizability model concerns the components of the polarizability tensor: $\alpha_{xx,A}$ and $\alpha_{xy,A}$ (in backscattering geometry light is incident along [001] and there are only E_x and E_y). On the assumption that $\partial\alpha_\perp/\partial l \ll \partial\alpha_\parallel/\partial l$, where $\alpha_\perp$ and $\alpha_\parallel$ are the polarizability components defined in the local bond coordinates and l is the bond length, it is found that $\alpha_{xx,A} \approx \alpha_{xy,A} = \alpha_A$.[16] For simplicity, α_{CdSe} and α_{CdTe} are neglected, which is reasonable as the vibrational amplitudes of Cd-Se and Cd-Te bonds are much smaller than those of Zn-Se bonds (LIF, LIF_2) and Zn-Te bond (LO_T). It is also consistent with the excitation lines of the Ar^+ laser where the Raman scattering efficiency of CdSe is much smaller than that of ZnTe.[1] Therefore only one variable, $\alpha_{ZnSe}/\alpha_{ZnTe}$, is required to calculate the relative scattering intensities of LIF, LIF_2, and LO_1.

Figure 3 shows relative intensities I_{LIF_2}/I_{LIF} and I_{LO_1}/I_{LIF} in the $z(x',x')\bar{z}$ configuration of $(\underline{Cd}Se)_4/(ZnTe)_8$ SL, where x' is parallel to the plane, say (110), containing a single Zn-Se WB for optimal LIF observation.[10] As the polarizability ratio ($\alpha_{ZnSe}/\alpha_{ZnTe}$) increases, I_{LO_1}/I_{LIF} decreases steadily owing to the confinement of LO_1 in ZnTe layers. However I_{LIF_2}/I_{LIF} has a quite different dependence. As $\alpha_{ZnSe} \sim \alpha_{ZnTe}$, the I_{LIF_2}/I_{LIF} value depends significantly on the configurations. As $\alpha_{ZnSe} > \alpha_{ZnTe}$, I_{LIF_2} of all configurations comes close to I_{LIF} while I_{LO_1}/I_{LIF} falls below 1. It implies that LIF_2 can readily be detected in experiment to manifest rearrangement. As $\alpha_{ZnSe}/\alpha_{ZnTe}$ increases from 1 to 3, however, the I_{LIF_2}/I_{LIF} value of the configuration R_2 and R_4 decreases but those of R_1 and R_3 behave oppositely. This is related to the peculiar interface structure of each rearrangement configuration, i.e., the Zn-Se double WB has Te ions as nearest neighbors (to form Zn-Te bonds) in $R_{2,4}$ but Cd ions (to form Cd-Se bonds) in $R_{1,3}$ (Fig. 1). α_{ZnTe} is not negligible in the range from 1 to 3. In $R_{2,4}$ configurations the nearest Te ions that are situated inside the ZnTe layer form Zn-Te bonds in the $(\bar{1}10)$ plane, which contribute to the scattering of LIF_2 owing to incomplete localization and resulting in a larger LIF_2 intensity. The Zn-Te bond near the single Zn-Se WB has a negligible contribution to the LIF intensity, however, since it lies in the (110) plane vertical to x'.[10] As the polarizability ratio becomes large, i.e., α_{ZnSe} predominates, the influence of this environmental Zn-Te bond remains negligible and I_{LIF_2}/I_{LIF} in all configurations tends to a similar value. LIF_2 is thus shown to have an intensity comparable to LIF and is Raman identifiable.

Calculations for IFM's of $(CdSe)_4/(ZnTe)_8$ SL are expected to be applicable to other CdSe/ZnTe SL's with different number of layers as IMF's are strongly localized at the interfaces. Besides the double Zn-Se WB is similar to the double Ga-As WB in the III-V semiconductor structure, where an As or Ga monolayer (ML) is sandwiched between two Ga or As ML's periodically (a similar situation occurs in the double Al-As WB).[5] These IFM's were well resolved with distinct peaks. Reference 5 also paid special attention to the connection between the buffer temperature and the atomic diffusivity. It is reasonable to expect that the rearrangement IFM, originating from similar double WB's, is also a probe in the II-VI SL's.

Figure 4 shows simulated Raman spectra of $(CdSe)_4/(ZnTe)_8$ SL for configuration S and R_i $(i=1-4)$. Probable strain at the Zn-Se bond[11] makes $\alpha_{ZnSe}/\alpha_{ZnTe}$ different from the bulk value with a particular dependence on configuration. The polarizability ratio is therefore obtained by fitting the experimental I_{LO_1}/I_{LIF} value, 0.27, taking the

overlapping of LO_1 and LIF into consideration.[2] In Fig. 3 the horizontal line corresponding to the ratio value 0.27 intersects the five solid curves in the range 2.9–5.0, where I_{LO_1}/I_{LIF} varies slowly. In this range all configurations give similar LIF_2 intensity. Each line is broadened to a Lorentzian shape with a full width at half maximum (FWHM) of 6 cm^{-1} for LO_1 and 9 cm^{-1} for LIF (all experimental values). FWHM of 9 cm^{-1} is also used in LIF_2 for simulation. A sample with perfectly sharp interfaces produces a Raman spectrum with two peaks, LO_1 and LIF, but a sample with rearranged interfaces might show an extra LIF_2 peak in addition. The 13 cm^{-1} separation of LIF_2 from LIF, both with similar intensity, makes a distinct characterization.

V. RESULTS OF EXPERIMENTS, IMPROVEMENT OF THEORY, AND DISCUSSION

On the bottom of Fig. 4, the Raman spectrum of the ALE grown $(CdSe)_4/(ZnTe)_8$ SL excited by 501.7-nm line is also shown for comparison. The Raman spectrum of ALE grown SL is identical to the simulated *S* spectrum but lacks the characteristic LIF_2 of atomic rearrangement. The peak at 209 cm^{-1} is LO_1—the ZnTe confined mode, and that at 222 cm^{-1} is LIF—the single Zn-Se WB IFM.[1] LIF_2 at 235 cm^{-1} is missing. For the other two samples with different layers, identical results are obtained. The absence of the LIF_2 modes indicates that no atomic rearrangement is detected in this ALE grown $(CdSe)_4/(ZnTe)_8$ SL. This could be caused by insufficient double WB's or insufficient long-range ordering. In fact, it reminds us that Raman calculations are complicated and require many approximations as noted in the previous sections. The prerequisite of the linear-chain model[19] is an ideal lattice so that the reordering configurations and following calculations are extreme cases involving long-range ordering of double WB's that is unlikely to exist in general.

Raman spectra for MBE-grown samples under similar experimental conditions, but using excitation lines of 496.5 and 514.5 nm, are shown in Fig. 5. There are only two Raman bands—LO_1 at 210 cm^{-1} and LIF at higher frequency. The expected LIF_2 is still missing. The fairly strong and sharp IFM peak shifts to a higher frequency (from 218 cm^{-1} for M_1 to 223 cm^{-1} for M_4) while the position of LO_1 of the ZnTe confined mode is unchanged.

The double Zn-Se WB mode foretold by theory is missing. LO_1 is not much stronger than LIF, which is a characteristic of single Zn-Se WB also shown by the full curves in Fig. 3. These show that LIF should be ascribed to single Zn-Se WB. LIF is a strongly localized interface mode whose frequency is almost independent of structural parameters such as the layer numbers *m* and *n* in theoretical calculations. Therefore the frequency variation of this mode, in the range 218–223 cm^{-1}, could be caused by interface disorder resulting from interdiffusion and interface roughness due to faceting and islanding during growth. The noticeable frequency shift of IFM in *AB*/*CD* SL's caused by interface disorder has been verified both theoretically[20] and experimentally.[4] The frequency shift of a sample is correlated to its spatial coherence length as measured in XRD.[1] The smaller the spatial conherence length, the larger the frequency shift. Interface disorder upshifts the frequency of IFM. Hence it is possible to separate the effect of interface disorder from that of interface reordering. The frequency shift in the Raman mode manifests the former and the appearance of a new IFM of double WB show the latter.

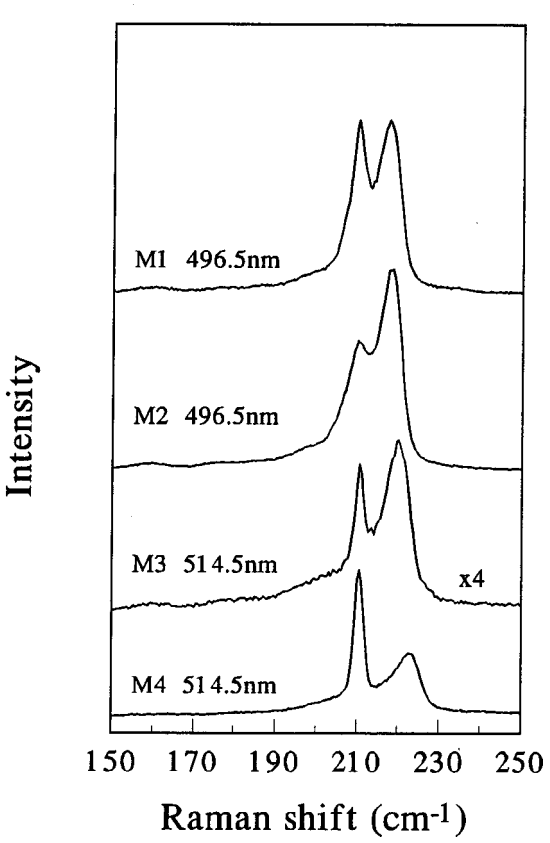

FIG. 5. Raman spectra of MBE $(CdSe)_m(ZnTe)_n$ SL's: M_1, $m=n=6$; M_2, $m=n=4$; M_3, $m=5$ and $n=3$; M_4, $m=n=2$. They are measured in $z(x',x')\bar{z}$ backscattering configuration.

This gives a clue to the discrepancy between experimental and theoretical frequencies of LIF: the LIF of M_1 and M_2 is ~ 4 cm^{-1} smaller than the value 222 cm^{-1} obtained from the linear-chain model. The expansion of interface Zn-Se bonds found by XAFS (Ref. 11) shows that the model constants require more realistic consideration. The input-bulk-value force constant is therefore considered as a zeroth-order approximation and reiterative calculations are then adopted to improve the theoretical results. A force constant 0.635 $\times 10^5$ dyn/cm for the Zn-Se interface bond, obtained by fitting to the LIF 218 cm^{-1} frequency of samples M_1 and M_2 [better quality shown by XRD (Ref. 11)], is used, which is 7.4% smaller than the bulk value for CdSe. Correspondingly, the calculated value of the LIF_2 position shifts to 228 cm^{-1}.

The question remains as to whether the LIF_2 of the interface rearrangement could appear. Characterization of MBE samples by XAFS shows that the Zn coordination number of Se ions and the Cd number of Te ions are larger than those expected from SL with sharp interfaces.[11] If we take M_2 and the coordination number of Se for example, there are 3.5 Cd and 0.5 Zn around Se on the average layer on a sharp interface (*S* configuration) but XAFS gives 2.30 ± 0.25 Cd and 1.70 ± 0.25 Zn instead. The average number of Zn-Se bonds

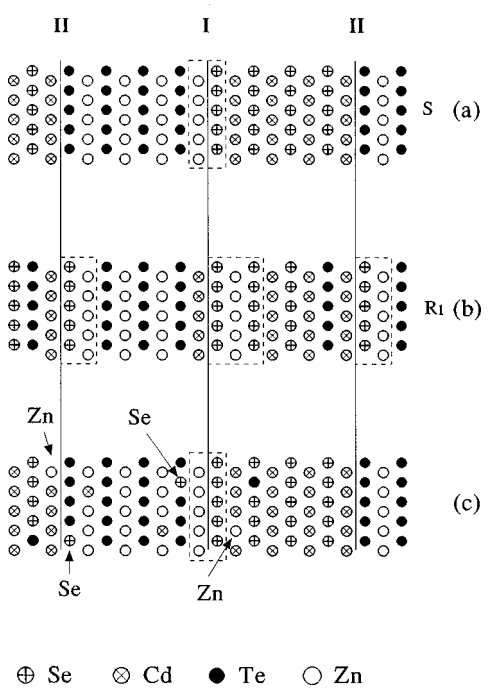

FIG. 6. Schematic cross section of $(CdSe)_4/(ZnTe)_8$ SL along the growth direction [001]: (a) with sharp interfaces; (b) configuration R_i; and (c) with interdiffusion of Zn and Se atoms into opposite layers.

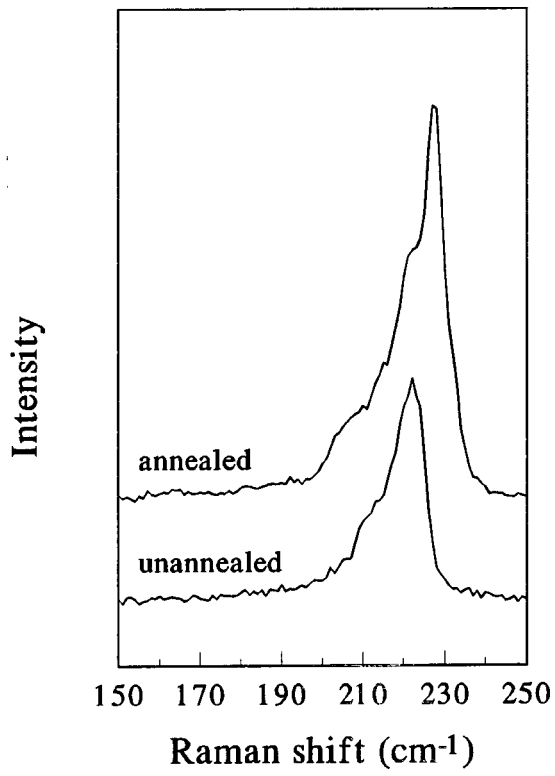

FIG. 7. Raman spectra of annealed and unannealed ALE $(CdSe)_4/(ZnTe)_8$ SL's measured in $z(x',x')\bar{z}$ backscattering configuration with 488.0 nm excitation.

is thus greater than expected. This could result from atomic reordering, as shown in Fig. 6(b) for the R_1 configuration, where previous single Zn-Se WB's become double Zn-Se WB's on interface I and additional single Zn-Se WB's are generated at interface II. There are now 1.5 Zn around Se. For the other three configurations there are similar changes. On the other hand, interlayer diffusion can result in the same increase of the average Zn number around Se [Fig. 6(c)], which is not so rigorous as the atomic reordering. The interlayer diffusion (or more simply disorder) has been observed by TEM on interfaces of two to three monolayers.[21] Although the interdiffusion origin is excluded in Ref. 11, observation by TEM and Raman scattering (frequency shift of LIF) show that the atomic reordering and interface disorder should be considered together. Theoretical calculations could exaggerate the situation of the double Zn-Se WB's based on the sole effect of atomic rearrangement. If interdiffusion is included, as shown by Fig. 6(c), some double Zn-Se WB's are locally formed, randomly distributed and thus lacking long-range ordering. Their only effect is on the position and profile of LIF (Ref. 20) but without LIF_2. It should be noted that the limited penetration depth of a visible laser beam in such opaque samples makes Raman scattering less sensitive to interfacial reordering than x-ray techniques. The absence of LIF_2 in the Raman spectra is ascribed to the lack of sufficient double Zn-Se bonds with long-range order. The growth temperature (220 °C for ALE and 310 °C for MBE) cannot generate enough Zn-Se double WB's with long-range order for Raman identification. To identify LIF_2, sufficient atomic rearrangement should be induced by, e.g., heat processing.

To examine this idea, several ALE-grown $(CdSe)_4/(ZnTe)_8$ samples, annealed at 410 °C for different times, have been studied. The one annealed for the longest time, 20 min, is found to exhibit an additional band on the high-frequency side at 227 cm^{-1} using 488.0-nm excitation (Fig. 7). In this case the LIF peak becomes a shoulder peak without any frequency change. The invariance of the LIF position shows that the effect of disorder is negligible. It could not be a coupled LO-plasmon mode since the carrier density is too low to produce any noticeable effect as in as-grown samples. Compared with the 228 cm^{-1} line of LIF_2 from the improved theoretical calculations, this additional feature at 227 cm^{-1} is identified as LIF_2 of double Zn-Se WB's. The new interfacial-reordering mode LIF_2 does exist as predicted by the theoretical models but the interfacial structure it reflects only appears after annealing.

It is shown that the LIF_2 mode can be observed in annealed samples. Preliminary studies on the annealed MBE samples result in the same observation of LIF_2. It will be highly interesting to investigate the progression of the spectrum with both annealing time and temperature to clarify the conditions of the development of LIF_2. We leave it for further study.

Further questions to consider are why the LO_1 mode does not appear and why the intensity of LIF_2 is much larger than LIF (Fig. 7). Theoretical calculations show that their intensities should be similar as LO_1 is much weaker (Fig. 4) but experimental results show a very strong dependence of the intensities of LO_1, LIF, and LIF_2 to the excitation wavelengths. The discrepancy is likely due to the effect of resonance. Figure 8 shows the Raman spectra of an unannealed ALE sample with different excitation lines at 77 K. With 457.9-nm excitation both LO_1 and LIF are almost unde-

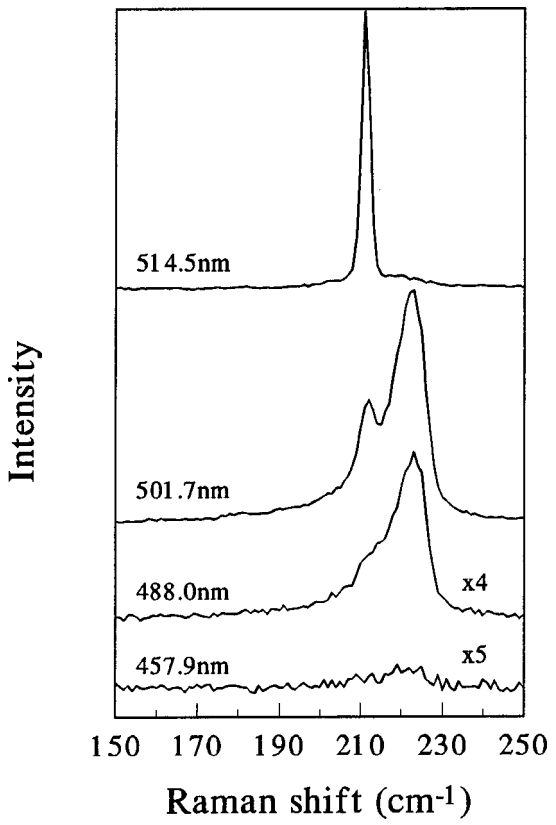

FIG. 8. Raman spectra of ALE sample, $(CdSe)_4/(ZnTe)_8$ SL, excited with different lines in $z(x',x')\overline{z}$ backscattering configuration. The top spectrum with 514.5-nm excitation is measured with both reduced laser power and reduced entrance slit.

tectable. As the wavelength increases to 488.0 and 501.7 nm, both LO_1 and LIF are significantly enhanced and the spectrum at 501.7 nm is close to the calculated results. In the spectrum with 514.5 nm excitation, however, the LO_1 mode has such huge enhancement that both the excitation power and the width of entrance slit have to be reduced to protect the detection electronics. LIF, on the contrary, is not enhanced so drastically. This is due to the fact that LO_1 is a confined mode within ZnTe layers whose energy gap (2.4 eV–517 nm) is very close to the excitation but LIF is localized at interfaces. The annealed sample shows similar wavelength sensitivity of the LO_1 intensity with respect to those of LIF and LIF_2. However, the relative intensities of LIF and LIF_2 first depend on the annealing conditions instead of the excitation wavelength. The much stronger line of LIF_2 compared with LIF (Fig. 7) also shows that assuming a single value for α_{ZnSe} for both single and double Zn-Se WB's is likely to be an oversimplification, considering their different sites, interface neighbors, and subsequent resonance effects. We leave this for further investigation.

We can make a rough estimate of the number of interfaces required for experimental observation of the IFM. The relative intensity of the IFM at $\sim 220\ cm^{-1}$ of CdSe/ZnTe SL's decreases when the period thickness of the superlattices increases as shown by Fig. 2 of Ref. 1. Sample $S1$ is $(CdSe)_4/(ZnTe)_8$ of 80 periods and sample $S2$ is $(CdSe)_8/(ZnTe)_{12}$ of 35 periods. As both samples are excited by the 4880-Å (2.55 eV) line, the IFM of $S1$ has a relative intensity almost twice as large as that of $S2$. The IFM intensity of $S3$, the $(CdSe)_{10}/(ZnTe)_{10}$ sample with 35 periods, is similar to $S2$. We assume that it results essentially from the decrease of total interfaces that can be illuminated by light rather than from the decrease of the volume fraction of the interfacial region. Considering the energy gaps, $E_g(ZnTe)=2.26$ eV and $E_g(CdSe)=1.74$ eV, and the absorption coefficient $\alpha(cm^{-1})=-4\times10^4[(h\nu-E_g)(eV)]^{1/2}$,[22] an estimate can be made that $\alpha(cm^{-1})$ at 2.55 eV excitation are 3.59×10^4 and 2.14×10^4 (all in units of cm^{-1}) for CdSe and ZnTe, respectively, although it is expected that their practical value might be larger owing to the big difference between $h\nu$ and E_g, interface reflection, and so on. Then the transmission depth determined by $1/\alpha$ could be found to be 52, 30, and 29 periods for $S1$, $S2$, and $S3$, respectively. The IFM signal from samples with periods thicker than $S2$ or $S3$ (e.g., $m=n=12$) and with similar 30 periods weakens so much that it can hardly be detected. Hence, the number of interfaces required for experimental observation of IFM is more than 30. The thickness of the CdSe layer is more crucial since $\alpha(CdSe)>\alpha(ZnTe)$ and this number also depends on excitation frequency and the quality of interfaces. This limit shows also in other cases, e.g., the IFM signal with 4579 Å (2.71 eV) excitation disappears in CdSe/ZnTe SL's with periods of 40.0 Å CdSe+163.1 Å ZnTe and 66.4 Å CdSe+16.6 Å ZnTe, respectively (Fig. 2 of Ref. 23). The estimate penetration depth of light is $\sim$17 and 32 periods, respectively. It seems that 30 periods or pairs of interfaces for observation of the IFM is a good estimate. Obviously we cannot observe the IFM in a simple heterojunction, which again stresses the importance of long-range order.

VI. CONCLUSIONS

In summary, theoretical calculations based on the linear-chain model predict a characteristic IFM for all configurations of atomic rearrangement that originate from double Zn-Se WB's. This additional feature on the high-frequency side of LIF is detectable with comparable intensity. Although experimental work on both ALE and MBE grown CdSe/ZnTe SL's show that no atomic exchange between layers of CdSe and ZnTe could be detected, the predicted LIF_2 indeed appears with strong intensity after annealing for 20 min at 410 °C (above both ALE and MBE growth temperatures). The theoretical models, though approximate and simplified, are thus shown to be applicable with limit. Experiments also show that Raman scattering can separate the effect of disorder from reordering.

ACKNOWLEDGMENTS

We are grateful to Professor J. Li and Professor S. X. Yuan of Shanghai Institute of Technical Physics, Academia Sinica, Shanghai, P.R. China, for providing the ALE samples, and to Professor J. K. Furdyna and Dr. G. L. Yang for providing the MBE samples.

[1] Y. Jin, Y. T. Hou, Shu-Lin Zhang, J. Li, S. X. Yuan, and G. G. Qin, Phys. Rev. B **45**, 12 141 (1992).
[2] S. L. Zhang, C. L. Yang, Y. T. Hou, Y. Jin, Z. L. Peng, J. Li, and S. X. Yuan, Phys. Rev. B **52**, 1477 (1995).
[3] I. Seal, L. A. Samoska, C. R. Bolognesi, A. C. Gossard, and H. Kroemer, Phys. Rev. B **46**, 7200 (1992).
[4] B. V. Shanabrook, B. R. Bennett, and R. J. Wagner, Phys. Rev. B **48**, 17 172 (1993).
[5] B. V. Shanabrook and B. R. Bennett, Phys. Rev. B **50**, 1695 (1994).
[6] D. Behr, J. Wagner, J. Schmitz, N. Herres, J. D. Ralston, P. Koidl, M. Ramsteiner, L. Schrottke, and G. Jungk, Appl. Phys. Lett. **65**, 2972 (1994).
[7] I. Sela, C. R. Bolognesi, L. A. Samoska, and H. Kroemer, Appl. Phys. Lett. **60**, 3283 (1992).
[8] J. Spitzer, H. D. Fuchs, P. Etchegion, M. Ilg, M. Cardona, B. Brar, and H. Kroemer, Appl. Phys. Lett. **62**, 2274 (1993).
[9] J. Wagner, J. Schmitz, J. D. Ralston, and P. Koidl, Appl. Phys. Lett. **64**, 82 (1994).
[10] S. G. Lyapin, P. C. Klipstein, N. J. Mason, and P. J. Walker, Phys. Rev. Lett. **74**, 3285 (1995).
[11] K. M. Kemner, B. A. Bunker, A. J. Kropf, H. Luo, N. Samarth, J. K. Furdyna, M. R. Weidmann, and K. E. Newman, Phys. Rev. B **50**, 14 327 (1994).
[12] J. Li, L. He, W. Shan, X. Y. Cheng, and S. X. Yuan, J. Cryst. Growth **111**, 736 (1991); Jie Li, Shixin Yuan, J. Yin, and Shu-Lin Zhang (unpublished).
[13] C. Colvard, T. A. Gant, M. V. Klein, R. Merlin, R. Fisher, H. Morkoc, and A. C. Gossard, Phys. Rev. B **31**, 2080 (1985).
[14] D. J. Olego, P. M. Raccah, and J. P. Faurie, Phys. Rev. B **33**, 3819 (1986).
[15] D. J. Olego, K. Shahzad, D. A. Cammack, and H. Cornelissen, Phys. Rev. B **38**, 5554 (1988).
[16] B. Jusserand and M. Cardona, in *Light Scattering in Solids V* edited by M. Cardona and G. Guntherodt (Springer-Verlag, Berlin, 1989), p. 49.
[17] B. Zhu and K. A. Chao, Phys. Rev. B **36**, 4906 (1987).
[18] L. A. Farrow, J. M. Worlock, F. Turco-Sandroff, R. E. Nahory, R. Beserman, and D. M. Hwang, Phys. Rev. B **45**, 1231 (1992).
[19] C. Kittel, *Solid State Physics* (Wiley, New Delhi, 1977).
[20] D. Kechrakos and J. C. Inkson, Semicond. Sci. Technol. **6**, 155 (1991).
[21] H. Luo, N. Samarth, F. C. Zhang, A. Pareek, M. Dobrowolska, J. K. Furdyna, K. Mahalingam, N. Otsuka, W. C. Chou, A. Petrou, and S. B. Qadri, Appl. Phys. Lett. **58**, 1783 (1991).
[22] B. Sapoval and C. Hermann *Physics of Semiconductors* (Springer-Verlag, Berlin, 1993).
[23] R. Sugie, H. Ohta, H. Harima, and S. Nakashima, J. Appl. Phys. **80**, 5946 (1996).